Journal of American Science

Websites:
http://www.jofamericanscience.org
http://www.sciencepub.net

Emails:
editor@sciencepub.net
sciencepub@gmail.com

MARSLAND PRESS
Multidisciplinary Academic Journal Publisher

The crucial physical attributes and traits of nanomaterials

Ranjeet Singh

Associate Professor, Department of Physics, Govt. College for Women, Panchkula, Haryana (India)
Email: ranjeetghotra@gmail.com

Abstract: Recent research has given a great deal of attention to nanomaterials and nanotechnologies. As a result of the advancement of nanoscience, new physical properties and new methods in sample preparation and device manufacturing are evoked. This research involves experts from several academic disciplines, including physics, chemistry, material science, and mechanical and electrical engineering. This overview discusses numerous techniques for creating nanomaterials, such as insulators, semiconductors, and metals. We describe the unusual physical characteristics of the temperature dependence of resistivities, the linear and nonlinear optical spectra, the spin resonance spectra, and magnetic susceptibility measurements. We have established a new perspective on quantum tunnelling, quantum phase transition, surface effect, quantum size-effect confinement, and nonlinear susceptibility increases as a result of a variety of exciting and surprising observations. The foundation of nanoscience and nanotechnology is nanomaterials. Over the past few years, research and development activity in the vast and interdisciplinary field of nanostructure science and technology has exploded globally. It has the potential to fundamentally alter the processes used to make materials and products, as well as the variety and type of functionalities that may be accessible. It already has a large commercial influence, and this impact will undoubtedly grow in the future.
[Singh, R. **The crucial physical attributes and traits of nanomaterials.** *J Am Sci* 2023;19(1):35-43]. ISSN 1545-1003 (print); ISSN 2375-7264 (online). http://www.jofamericanscience.org. 05.doi:10.7537/marsjas190123.05.

Keyword: insulators, nanostructured catalysts, Nanoparticles, Metallic Nanoparticles, Silicon Single-electron Transistors

Introduction:

By vacuum evaporating iron in inert gas and condensing it on chilled substrates, the first nanomaterials were created [1]. After that, numerous techniques for creating nanoparticles, including those using inorganic ceramics and organic compounds, were developed. Examples include the use of an arc plasma torch to create metallic powder [2, 3], the laser-induced CVDM method to create unique compounds [4,] and microwave plasma enhanced CVD to create brittle, hard materials. Instead of chemical vapour, single-phase compounds can be produced via liquid co-precipitation [5] and single-phase oxide metals can be created by solid-state thermal breakdown [6]. There are some examples of specific techniques. The formation of nanostructures in the first meteorites marked the beginning of the history of nanomaterials shortly after the big bang. Many more nanostructures, including skeletons and seashells, were later developed by nature. Early humans' usage of fire resulted in the formation of smoke particles with a nanoscale. But the history of nanomaterials in science didn't start until much later. Michael Faraday's 1857 production of colloidal gold particles is one of the earliest reports in science. For more than 70 years, researchers have also studied nanostructured catalysts. Precipitated and fumed silica nanoparticles were being produced and offered as an alternative to ultrafine carbon black for rubber reinforcements in the USA and Germany by the early 1940s. Sample Preparation: After that, numerous techniques for creating nanoparticles, including those using organic and inorganic materials, were developed. These included the use of an arc plasma torch to create metallic powder [2, 3], the laser-induced chemical vapour deposition method (CVDM), which creates unique compounds [4,] and microwave plasma enhanced CVD, which creates brittle and hard materials. By vacuum evaporating iron in inert gas and condensing it on chilled substrates, the first nanomaterials were created [1]. After that, numerous techniques for creating nanoparticles, including those using inorganic ceramics and organic compounds, were developed. Examples include the use of an arc plasma torch to create metallic powder [2, 3], the laser-induced CVDM method to create unique compounds [4,] and microwave plasma enhanced CVD to create brittle,

hard materials. Chemical vapour is replaced by liquid co-precipitation.

Metallic Nanoparticles:

Metallic nanoparticles are prepared using a variety of techniques that elicit various properties for the intended uses. The techniques that are frequently used are: Sol-gel technique [7] For instance, etraethylorthosilicate (Si(OC2H54, TEOS), ethanol, and water are combined with an AgNO3 solution to create silver nanoparticles, which are subsequently catalysed by a few drops of HNO3. The blended mixture was spread out and dried. The dried gels were reduced at a temperature of 400 C for 30 min in hydrogen gas. The Ag particles have a size of about 5∼10 nm with a profile distribution in the form of lognormal distribution. The nanoparticles are embedded in silica glass in wellseparated and protected matrix. The preparation of iron nanoparticles embedded in glass can be prepared with the same method by substituting FeCl3 for the silver salt. The advantages of the sol-gel process include high purity, isotropic, and low temperature annealing, as well as a lack of breaking after drying with substantial doping. By using high temperature sintering, it is possible to eliminate the free water absorbed in the porous gel, the H O• bonds desorbed on the porous surface, or the chemically absorbed hydroxyl groups that alter the optical absorbance between 160 and 4500 nm.

Nanoparticles: Insulators

On earth, silicon dioxide is widely present. Quartz and fused silica are well-known names for the crystalline and non-crystalline forms of silicon dioxides, respectively. Since silica surfaces are crucial for catalysis, chemical processes, and the creation of microelectronic devices, the interface of amorphous silica has been well studied. For these widely used materials to be used in more practical ways, careful understanding of the optical characteristics of amorphous silica surfaces is essential.

Both silica nsnaospheres and silver nanoparticles have been prepared using the sol-gel method [16]. Salts are hydrolyzed in this process. By sintering at a temperature significantly lower than the system's liquid temperature, ultra pure or homogenous multi-component glasses can be created. Typically, the process starts with alkoxide molecules and proceeds through polycondensation and hydrolysis at room temperature. Tetraethylorthosilicate (TEOS), Si(OC2H5 4, ethanol, and water are one specific example. After stirring, the three reactants combine to create a single phase solution. Below is a diagram illustrating the basic reactions in the sol-gel process.

$$SiOC2H54 + 4H2O \rightarrow SiOH4 + 4C2H5OH$$

$$SiOH4 \rightarrow SiO2 + 2H2O$$

In order to ensure thorough hydrolysis, 4 to 20 mols of water are typically added per mol of TEOS. A sol is created when enough linked Si-O-Si connections develop in one area and interact with one another to create colloidal particles. The colloidal particles join together to form a three-dimensional network after sedimentation for several days. There have been numerous research on the impacts that adding an acid or base catalyses the process and results in gels with various morphologies and structures. Gelatin is created when acid-catalyzed (PH 2) linear polymers entangle with one another. More branch clusters are formed by base-catalyzed reactions (PH > 11). Acid-catalyzed gels are often transparent, whereas base-catalyzed solutions are typically murky. However, Karmakar et al. [21] employed acid-catalyzed TEOS to create glass-like silica microspheres with densities ranging from 2.10 to 2.16 g/cm3. The monodispersive spheres produced by the Stober technique are solid silica particles with pores. The microspheres range in size from 1060 m and above. Controlling the sizes and size distributions is challenging. Additionally, necks connect the particles to one another. By washing them with ethanol and acetone one after the other, they can be separated from one another. The production of silica submicrospheres and microspheres doped with Pr+3 and Er+3 was reported by Moran et al. in [22].

Quantum dot transistors or Semiconductor:

The pinnacle of semiconductor physics and the greatest challenge are presented by semiconductor quantum dots (QD) with tunable optical emission frequencies as a result of the quantum size confinement. It was possible to execute a modified Stranski-Krastanow growth process at the surface of a substantially strained heterostructure [24]. The GaAs substrate was covered with a thin layer of InAs using

the molecular beam epitaxy technique. The strain on the interface grows as the InAs film increases because to the 7% lattice mismatch between GaAs and InAs, which prompts a locally three-dimensional growth of InAs to relieve the strain. The produced defect-free quantum dots have a low laser threshold current and provide highly efficient light emission. A layer of InGaAs is typically formed on the surface of InAs to provide the emission wavelength, which is typically used in optical communication and ranges from 1.29 to 1.3 m. Quantum well patterning via lithography, which comprises the electron beam interference technique [25], focused ion beam lithography [26], optical lithography [27], and X-ray lithography [28], was thought to be the simplest method of QD production. Arrayed laser emission is an intriguing application for the self-organized nanodots with regulated size, defect-free, strong carrier localization, and quantum Stark effect production on strained hetero epitaxial surface.

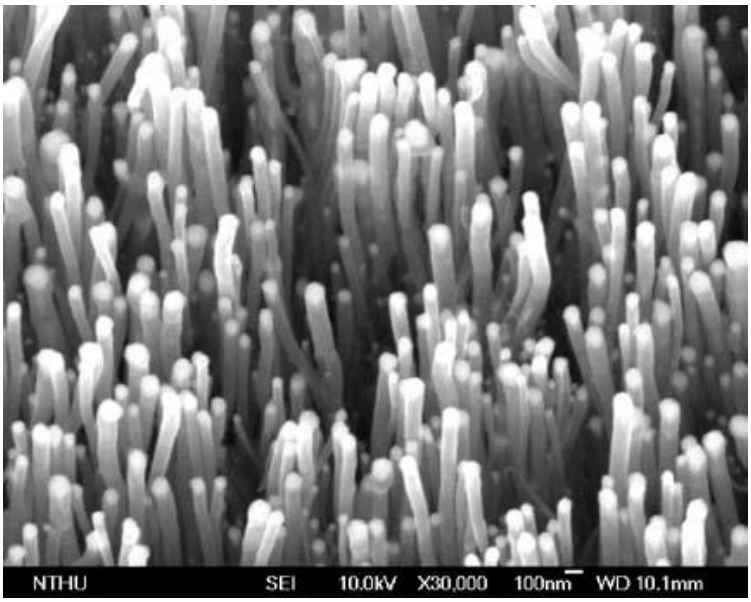

A nanowire and a nanotube:

Due to its outstanding stiffness, strength, elasticity, electric conductivity, and field emission properties, carbon nanotubes rank among the most promising materials lately produced. In this research, we focus on growing multi-wall carbon nanotubes for field emission on metallic surfaces, with the hope that they would find practical applications in displays and light lighting. The majority of substrates currently used for the chemical vapour deposition (CVD) process used to grow carbon nanotubes (CNTs) are silicon wafers coated with a thin layer of transition metal catalysts, where carbon is dissolved and then precipitated as hexagonally packed graphite on the cooling surface side. The actual growth outcome supports the controllability of the CNT's diameter under the growth conditions depicted above, with the exception of adjusting the growth period to 15 min and the RF selfbias to 450 V, and using an alloy substrate made up of Cu-10 wt% Fe-10 wt% Co-10 wt% Ni. On the dendrite, the CNTs grow precisely and uniformly, reaching a length of around 3 m. The increased growth of CNTs can be seen on the right side of Figure 4(a), where the dendritic density is higher due to the hydrogen etching of a larger concentration of iron-based components (Fe, Co, and Ni).

As illustrated in Figure 6, the proper sample was chosen through laborious and delicate SEM examination with just a single CNF appearing across the electrode gap (a). The CNF was multi-connected to be securely developed on the nickel electrodes (Fig. 6(b)), and as the electrode gap is decreased, it becomes much straighter with the disadvantage of developing many fibers. Longer than 1 m nanotubes are typically referred to as nanowires or nanofibers. They can be created using physics, chemistry, or a combination of the two to create semiconductors [59-61] and metallic wires [57, 58]. In porous alumina that has been improperly anodized, gold nanowires can be chemically deposited; the bare gold wire is then produced by wet etching the alumina [62].

Figure 4 shows the SEM of (a) well-aligned and thriving CNT growth on a Cu-10 wt% Fe-10 wt% Co-10 wt% substrate. Substratum made of bulk nickel alloy, and (b) an illustration of the right side of (a) displaying upright tubes embedded with catalyst particles at tips. Reprinted from [53], S. Y. Chen et al., J. Phys. D.: Appl. Phys. 37, 273, with permission (2003). Institute of Physics, 2003.

Illustrates how a laborious and sensitive process of the SEM picked the optimal sample with a single CNF presenting across the space between the electrodes (a). The CNF was multi-connected in order to be securely grown on the nickel electrodes (Fig. 6(b)), and as the electrode gap is decreased, it becomes more straighter with the disadvantage of developing multiple fibres. More than 1 m long nanotubes are typically referred to as nanowires or nanofibers. They can be created using physics, chemistry, or a combination of the two to create semiconductors [59-61] and metallic wires [57, 58]. In porous alumina that has been improperly anodized, gold nanowires can be chemically deposited; the bare gold wire is then produced by wet etching the alumina [62].

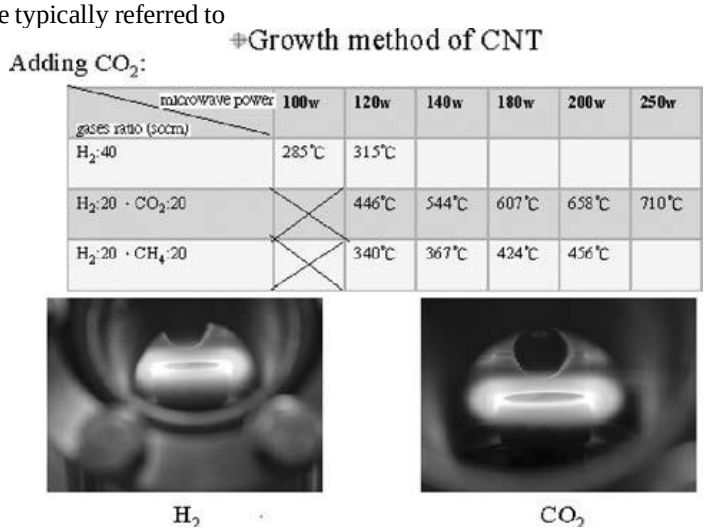

Figure 5 Illustrates the colours of the plasma balls for hydrogen and carbon dioxide flow gases on the left and right columns of Figure 4(a), respectively. Carbon dioxide flow can significantly raise the plasma temperature, turning it white. Reprinted with permission from J. Nanosci. Nanotechnol. 5, 1987; S. Y. Chen et al., [56]. (2005). American Scientific Publishers, 2005.

PHYSICAL PROPERTIES AND STRUCTURE:

Structures: With a spatial resolution of 0.2 m for Auger electron spectroscopy (AES) and 0.2 mm for X-ray photonelectron spectroscopy (XPS), and a sensitivity of 0.3% [70] for both analyzers, it is possible to describe the surface impurities to a depth of 0.5–1 nm. The crystal composition and structure can be easily seen in the TEM electron diffraction pattern and the powder X-ray diffraction pattern. By using the Scherer's equation and the equation provided by [71], it is possible to estimate the average grain size R for a known X-ray wavelength at the diffraction angle.

$$FWHM=0.94\lambda/R\ COS\theta$$

where R and are in nanometers, and the full width at half maximum (FWHM) of the typical spectrum is expressed in radians. The electron probe micro-analysis (EPMA) from a scanning electron microscope may quickly look at the impurity levels (SEM). By looking at the infrared absorption spectra, one can identify the chemical bonding modes that are linked to the metal particle surfaces. The development of carbon nanotubes [72] on a Cu-20 wt% Fe substrate using ammonia gas as an intake exposes a dense layer of cotton-like material. The appearance is a fluffy, more than 3-mm-thick, blue-purple structure. Figure 10's SEM image depicts a 500 nm-long filament that is incredibly fragile. As seen in Figure 11, we can compare the morphology of the HR-TEM and electron diffraction. The inset displays weak diffraction rings caused by polycrystalline metal particles that are implanted, with each spot made up of five sections that emerge from various-sized tubes. It clearly demonstrates the chiral structure, a tube diameter of around 25 nm, and 0.29 nm-wide longitudinal black-and-white striae.

Field Emission:

First, using an Astex 5400 microwave plasma enhanced chemical vapour deposition (MPECVD) system, polycrystalline boron-doped diamond sheets were produced on a p-type (100) oriented Si substrate. Previous report [87] provided a detailed description of the technique. The samples were installed on the cooling station of a helium closed-cycle refrigerator in order to evaluate the impact of temperature on the field emission. A 50 m Teflon spacer was used to separate the diamond layer from the indium-tin oxide coated glass anode. As the sample cooled down from room temperature to 20 K, typical measurements were taken. A current source that can be programmed offers output voltages that range from 0 to 1100 V while maintaining a stepwise constant current. as indicated by, emission current density

$$\mathbf{J_{total}} = Jc + Jv + J$$

where Jc, Jv, and Js are the emission current densities, and Tc, Tv, and Ts, respectively, are the tunnelling probabilities from the conduction band, valence band, and surface state. The WKB approximation is used. The current density is easily derived from the transmission probability [88] for electrons to tunnel through the potential barrier as given by Jc = AT 2TceqBnVs/KT, where A is the Richardson constant, Tc is the electron tunnelling coefficient, Bn is the n-type semiconductor's barrier height, and Vs is the applied voltage developed across the semiconductor. According to Bandis et al. [89], field emission from surface states is implausible, meaning that Js is insignificant. A painstaking modification to Eq. (1) can result in a straightforward formalism [90] as

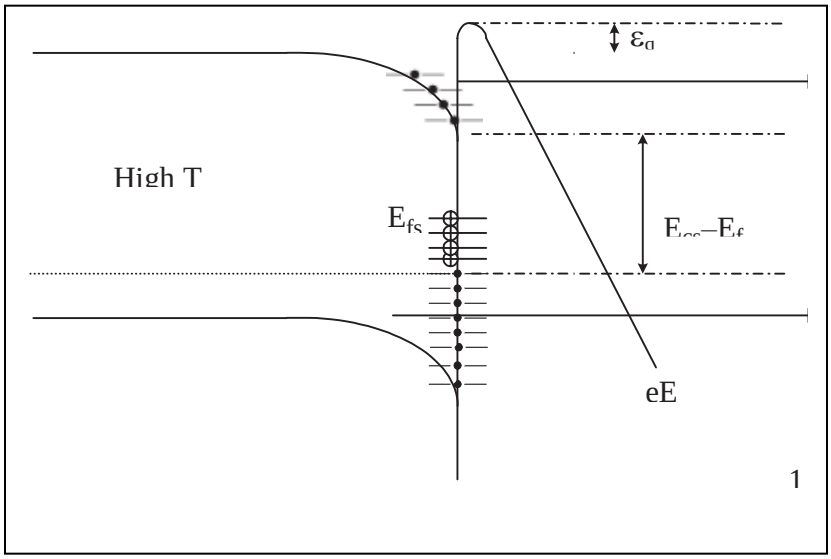

Figure: Theoretical fitting for B-doped diamond-like films with Ecs-Ef, the energy gap between surface conduction level and Fermi level, and y, the electron affinity. Reprinted with permission from [90], J. Non-Cryst. Solids 265, 230 by J. T. Lue et al (2000). © 2000.

The field emission current from the conduction band is heavily temperature dependent, whereas the valence band, which dominates the emission current at low temperatures and is negligibly small for p-type diamond and diamond-like films, has no dependency on temperature. The emission current at high fields and low temperatures can be addressed using the usual F-N equation.

Nonlinear Optics:

Non-Linear Optical Generation:

The phase matching condition is typically ignored for nanomaterials with particle size or film thickness much smaller than the coherent length, and the surface nonlinearity makes a noticeable contribution because of the improved surface to volume ratio. The existence of the nonlinear EZE source term, which makes a significant contribution at the boundary due to the discontinuity in the lattice structure, and the presence of the bulk magnetic dipole term E /H/t resulting from the Lorentz force of electrons were used to establish surface second harmonic generation (SHG) from metals. There have been numerous motivated theoretical and experimental SHG studies of bulk metals presented up to this point [315-318] that continue to draw a lot of interest. Accordingly, the Rudnick and Stern [317] provided phenomenological parameters a and b were used to construct and modify the theory of SHG from metal surfaces to express the components of current density that are normal and parallel to the surface, respectively. However, there are still few discussions of azimuthally scanned SHG that depend on the interaction between metal films and the production of nanoparticles on silicon substrate [319]. The electric quadruple field located in the selvedge area is the primary source for the creation of second harmonic light for metal particles with inversion symmetry [320-322]. Thus, a key tactic for improving second harmonic generation is the activation of surface plasmons (SP), which couple the incident field to travel along the surface. The electromagnetic waves' momentum conservation and very small wave-vector bandwidth determine how well surface plasmons are generated. The phase matching criterion is pursued by the light scattered from the many nanoparticles in a random orientation. Second harmonic generation (SHG) intensity reflected from metallic island films has recently been reported to have increased significantly [323-325].

NANODEVICES:

Silicon Single-electron Transistors and Electron:

The metal single electron transistor (SET), utilising the Coulomb blocket effect, has been swiftly developed to lower the size of current devices beyond the limit of one hundred nm. It is anticipated that conventional semiconductor logic or analogue devices will be replaced by devices that have been scaled down to atomic scale. Tunneling current easily outperforms the traditional conduction currents as a result of the isolated gate's distance from the drain and source being reduced to several nanometers. Due to the incredibly small capacitance of the gate, the tunnelling of a single electron to it can result in a significant potential drop. Due to the forward and backward scattering of electrons, the distribution of exposure intensity exhibits a Gaussian intensity profile. The two major ways to counteract proximity effects are to either predict changes in the features' dimensions and make compensating adjustments beforehand, or to modify the dosage of electron beams in accordance with the density of the patterns. However, this paper describes the creation of single electron transistors (SETs), which were produced by subjecting various patterns' forms to incident electrons of various intensities.

Surface Modification by Electric Discharge with Electrodes Implemented with Carbon Nanotubes:

We show that using multi-wall carbon nanotubes may produce a fine pattern using a promising nanofabrication technique (MWCNT). As miniature electrodes to oxidise silicon nitrite with the benefits of long-life, MWCNTs were grown on a tungsten tip using the hot-filament chemical-vapor deposition method (see Fig. 60). As shown in Figure 61, the MWCNTs are arranged into arbitrary arrays by computer controlling a 3D step motor on which the tungsten tip is loaded. A study of surface plasmon polariton [SPP] resonance enhancement utilising the Kretchmann configuration to find the 2D photonic crystal's dielectric characteristics is shown. Illustrate, respectively, the surface alterations of the n-type Si substrate [354] before and after the electric discharge machining (EDM) under a pressure of 103 torr. An improvement in surface roughness to 600 nm is readily visible after a 20-minute nanoscaled EDM polishing process. The rate of surface elimination for the nano-scale EDM polishing process using the MWCNTs cathode is 30 nm/min. Recent advancements in near field scanning optical microscopy (NSOM) offer a novel method for obtaining optical pictures with great spatial resolution that are not diffraction-limited.The diffraction limit of far-field optics is being overcome by near-field optical techniques using evanescent light because they create small spot sizes, and they have been used in nanofabrication. In this instance, a solid immersion lens (SIL), scattering points, or a narrow aperture have been utilised to capture or retrieve minuscule marks past the diffraction limit [355-362].

CONCLUSIONS:

In this overview, we've shown how to make nanoparticles using insulators, semiconductors, carbon nanotubes, metals, and magnetic ferrofluids, among other materials. Aligned and randomly aligned carbon nanotubes were produced on copper-based iron alloys using the microwave-enhanced plasma CVD method and radio frequency-induced self-bias hot-filament method, respectively. The semiconductor thermionic emission theory effectively expresses the temperature dependency on the field emission of CNTs. There is a brief description of the physical characteristics of nanomaterials, including structure, electrical and magnetic properties, linear optical and nonlinear optical properties due to classical size and quantum size effects. Nano-ferro fluid behaviour in the unique quantum phase transition is illustrated. Within the microwave frequency ranges, metallic nanoparticles' dielectric constants are determined. The use of nanofabrication to handle nanodevices is described. In this scenario evaluation, it is not possible to meticulously detail every aspect of this freshly created sophisticated system.

REFERENCES:

[1]. A. Roosen and H. Hausner, “Cermanic Powders.” Elsevier, Amserdam, 1983.
[2]. J. Eckert, J. C. Halzer, and C. E. Krill III, J. Appl. Phys. 73, 2794 (1993).
[3]. S. K. Ma and J. T. Lue, Solid State Commun. 97, 979 (1996).
[4]. W. Stober, A. Fink, and E. J. Bohn, J. Colloid Interf. Sci. 26, 62 (1968).
[5]. S. P. Mukherjee, “Sol–Gel Technology for Thin Films, Fibers, Preforms, Rlrctronics and Specialty Shapes” (I. C. Klein, Ed.). Noyes Pub., Park Ridge, New York, 1988.
[6]. T. Lopez, J. Mendez, T. Z. Mudio, and M. Villa, Mater. Chem. Phys. 30, 161 (1992).
[7]. R. F. Marzke and W. S. Glaunsinger, Proceedings of the Symposium on the Characterization of Materials with Submicron Dimensions, Philladelphia, (1983).
[8]. R. V. Upadhyay, D. Srinivas, and R. V. Mehta, J. Magn Magn. Mater. 214, 105 (2000).
[9]. V. K. Sharma and F. Waldner, J. Appl. Phys.

48, 4298 (1977).
[10]. R. E. Cavicchi and R. H. Silsbee, Phys. Rev. Lett. 52, 1453 (1984).
[11]. F. Frank, W. Schulze, B. Tesche, J. Urban, and B. Winter, Surf. Sci. 156, 90 (1985).
[12]. L. C. Klein, "Sol–Gel Technology for Thin Films, fibers, Preforms, Electronics, and Specialty Shapes." Noyes Publications, 1988; C. J. Brinker and G. W. Scherer, "Sol–Gel Science." Academic Press, San Diego, 1990
[13]. Gleiter, Progress in Meter. Sci. 33, 323 (1989).
[14]. K. Tanaka, K. Ishizaki, and M. Uda, J. Mater. Sci. 22, 2192 (1987).
[15]. J. S. Haggerty, W. R. Cannon, and J. I. Steinfewld, "Laser Induced Chemical Process." Plenum Press, New York, 1981.
[16]. A. Roosen and H. Hausner, "Cermanic Powders." Elsevier, Amserdam, 1983.
[17]. T. C. Edwards, "Foundations for Microstrip Circuit Design." John Wiley & sons, New York, 1983.
[18]. D. Spenato, A. Fessant, J. Gieraltowski, J. Loaec, and H. Legall,J. Magn. Magn. Mater. 140, 1979 (1995).
[19]. N. Vukadinovic, M. Labrune, J. Ben Youssef, A. Marty, J. C. Toussaint, and H. Le Gall, Phys. Rev. B 65 (2002).
[20]. Soshin Chikazumi, "Physics of Magneticm" (S. H. Charap, English Ed.), p 338. (1966).
[21]. George Rado, "Magnetism." Academic press, Vol. 1, p. 465.
[22]. B. Heinrich, "Ultrathin Magnetic Structure." Springer-Verlag, Berlin, 1994, p. 216.
[23]. C. Kittel, "Introduction to Solid State Physics." John Wiley & Sons, New York, 1986, p. 480, 6th edn.
[24]. S. Chikazumi, "Physics of Magnetism" (Stanley H. Charap, Ed.), p. 138. (1966).
[25]. H. A. Wheeler, IEEE Trans. MTT-25, 631 (1977).
[26]. W. J. Getsinger, IEEE Trans. MTT-21, 34 (1973).
[27]. M. Kobayashi, IEEE Trans. Microwave Theory Tech. MTT-30, 2057 (1982).
[28]. R. A. Pucel et al., IEEE trans. MTT, MTT-16, 342 (1968).
[29]. S. W. Chang, J. H. Liua, and J. T. Lue, Meas. Sci. Technol. 14, 583 (2003).
[30]. A. Dubey, etc., Electron. Lett. 37, 1296 (2001).
[31]. W. P. Halperin, Rev. Modern Phys. 58, 533 (1986).
[32]. W. C. Huang and J. T. Lue, J. Chem. Solids 58, 1529 (1997).
[33]. J. T. Lue, W. C. Huang, and S. K. Ma, Phys. Rev. B 51, 14570 (1995).
[34]. W. C. Huang and J. T. Lue, Phys. Rev. B 59, 69 (1999).
[35]. Berger, J. Kliava, J. C. Bissey, and V. Baietto, J. Appl. Phys. 87, 7389 (2000).
[36]. L. Zhang, G. C. Papaefthymiou, and J. Y. Ying, J. Appl. Phys. 81, 6892 (1997).
[37]. K. Y. Lo and J. T. Lue, Phys. Rev. B 51, 2467 (1995).
[38]. S. A. Carter, T. F. Rosenbaum, J. M. Honig, and J. Spalek, Phys. Rev. Lett. 67, 3440 (1991); Phys. Rev. B 48, 16841 (1993).
[39]. H. V. Lohneysen, T. Pietrus, G. Portisch, H. G. Schlager,A. Schroder, M. Sieck, and T. Trappmann, Phys. Rev. Lett. 72, 3262 (1994); B. Bogenberger and H. V. Lohneysen, ibid 74, 1016 (1995).
[40]. M. B. Maple, C. L. Seaman, D. A. Gajewski, Y. Dalichaouch, V. B. Barbetta, M. C. de Andrade, H. A. Mook, H. G. Lukefahr, O. O. Berna, and D. E. MacLaughlin, J. Low. Temp. Phys. 99, 223 (1995).
[41]. S. Chakravarty, B. I. Halperin, and D. R. Nelson, Phys. Rev. B 39, 2344 (1989).
[42]. S. Sachdev and J. Ye, Phys. Rev. Lett. 69, 2411 (1992).
[43]. J. Miller and D. A. Huse, Phys. Rev. Lett. 70, 3147 (1993).
[44]. J. T. Lue, W. C. Huang, and S. K. Ma, Phys. Rev. B 51, 14570 (1995).
[45]. E. M. Chudnovsky and J. Tejada, "Macroscopic Quantum Tunnel- ing of the Magnetic Moment." Cambridge, 1998, p. 94.
[46]. C. Paulsen, L. C. Sampaio, R. Tachoueres, B. Barbara, D. Fruchart, A. Marchand, J. L. Tholence, and M. Uehara, J. Magn. Magn. Mater. 116, 67 (1992).
[47]. X. X. Zhang, J. M. Hernandez, J. Tejada, and R. F. Ziolo Phys. Rev. B 54, 4101 (1996).
[48]. J. Tejada, L. Balcells, S. Linderoth, R. Perzynski, B. Barbara, and J. C. Bacri, J. Appl. Phys. 73, 6952 (1993).
[49]. R. H. Kodama, C. L. Seaman, A. E. Berkowitz, and M. B. Maple,J. Appl. Phys. 75, 5639 (1994).
[50]. C. T. Hsieh, C. C. Liu, and J. T. Lue, Appl. Surf. Sci. 252, 1899 (2005).
[51]. R. H. Kodama, A. E. Berkowitz, E. J. McNiff, Jr., and S. Foner,Phys. Rev. Lett. 77, 394 (1996).
[52]. S. Sachdev, "Quantum Phase Transitions." Cambridge, 1999, p. 8.
[53]. C. T. Hsieh and J. T. Lue, Phys. Lett. A 36,

329 (2003).
[54]. A. Garvin and C. L. Chien, J. Appl. Phys. 67, 938 (1990).
[55]. G. Xiao, S. H. Liou, A. Levy, J. N. Taylor, and C. L. Chien, Phys. Rev. B 34, 7573 (1986).
[56]. V. K. Sharma and A. Baiker, J. Chem. Phys. 75, 5596 (1981); C. T. Hseih, W. L. Huang, and J. T. Lue, J. Phys. Chem. Solids 63, 733 (2002).
[57]. R. S. de Biasi and T. C. Devezas, J. Appl. Phys. 49, 2466 (1978).
[58]. C. T. Hsieh and J. T. Lue, European J. Phys. B 35, 357 (2003); C. T. Hsieh and J. T. Lue, Phys. Lett. A 300, 636 (2002).
[59]. M. Stampanoni, A. Vaterlaus, M. Aeschlimann, and F. Meier, Phys. Rev. Lett. 59, 2483 (1987).
[60]. B. N. Engle, C. D. England, R. A. Van Leeuwen, M. H. Wiedemann, and C. M. Falco, Phys. Rev. Lett. 67, 1910 (1991).
[61]. F. J. A. de Broeder, D. Kuiper, A. P. Van de Mosselaer, and
[62]. W. Hoving, Phys. Rev. Lett. 60, 2769 (1988).G. Bochi, H. J. Hug, D. I. Paul, B. Stiefel, A. Moser, I. Parashikov, H.-J. Guntherodt, and R. C. O'Handley, Phys. Rev. Lett. 75, 1839 (1995).
[63]. L. Prejbeanu, L. D. Buda, U. Ebels, and K. Ounadjela, Appl. Phys. Lett. 77, 3066 (2000).
[64]. H. N. Lin, Y. H. Chiou, B. M. Chen, H. P. D. Shieh, and Ching- Ray Chang, J. Appl. Phys. 83, 4997 (1998).
[65]. M. Lohndorf, A. Wadas, H. A. M. van den Berg, and W. Wiesen- danger, Appl. Phys. Lett. 68, 3635 (1996).
[66]. H. S. Cho, C. Hou, M. Sun, and H. Fujiwara, J. Appl. Phys. 85, 5160 (1999)
[67]. L. J. Heyderman, H. Niedoba, H. O. Gupta, and I. B. Puchalska,J. Magn. Magn. Mater. 96, 125 (1991).
[68]. S. Chikazumi, "Physics of Magnetism, John-Wiley Series on the Science and Technology of Materials." New York, 1964, p. 238.
[69]. C. T. Hsieh and J. T. Lue, Appl. Surf. Sci. 252, 1899 (2005).
[70]. M. Pratzer, H. J. Elmers, M. Bode, O. Pietzsch, A. Kubertzka, and R. Wiesendanger, Phys. Rev. Lett. 87, 12701 (2001).
[71]. T. C. Choy, "Effective Medium Theory: Principles and Applica- tions." Oxford University Press, New York, 1999.